

# Stress–strain response in human dentine: rethinking fracture predilection in postcore restored teeth

Kishen A, Kumar GV, Chen N-N. Stress–strain response in human dentine: rethinking fracture predilection in postcore restored teeth. *Dent Traumatol* 2004; 20: 90–100. © Blackwell Munksgaard, 2004.

**Abstract** – In this study, the biomechanical perspective of fracture predilection in post-core restored teeth is investigated using computational, experimental, and fractographic analyses. The computational finite element analysis and the experimental tensile testing are used to evaluate the stress–strain response in structural dentine. The fractographic evaluations are conducted using laser scanning confocal microscopy and scanning electron microscopy to examine the topography of dentine from experimentally fractured specimens, and clinically fractured post-core restored teeth specimens. These experiments aided in correlating the stress–strain response in structural dentine with cracks and catastrophic fractures in post-core restored teeth. It was observed from these experiments that the inner dentine displayed distinctly high strains (deformations), while the outer dentine demonstrated high stresses during tensile loading. This implies that the energy fed into the material as it is extended will be spread throughout the inner dentine, and there is less possibility of local increase in stress at the outer dentine, which can lead to the failure of dentine structure. During post-endodontic restoration with increase in loss of inner dentine, the fracture resistance factor contributed by the inner dentine is compromised, and this in turn predisposes the tooth to catastrophic fracture.

It has been an empirical clinical observation that teeth are more prone to fracture as increasing amounts of tooth structure are lost from disease or operative procedures (1–3). Although evaluation of moisture loss, physical properties and biomechanical properties of dentine from endodontically treated teeth revealed no significant difference from non-endodontically treated teeth (4–6), different static, dynamic, and fracture resistance analyses have emphasized that loss of dentine is the primary cause for fracture susceptibility in endodontically treated teeth (7–9). The fracture resistance studies presented numerical values that can be used to compare effectiveness of one restorative procedure over the other. However, they did not offer any understanding on how dentine structure adapts

naturally to resist catastrophic fractures. This understanding is crucial for the restoration of a structurally compromised tooth to its ‘original’ status.

The fracture behavior of biologic material such as dentine is complex and is relatively unexplored. In most of the earlier attempts to produce a theory of fracture, one of the objectives has been to produce single numerical values, which are material parameter (10, 11). In the case of dentine that exhibits complex material property distribution, and unique mechanical response to deformation, the usefulness of these values is questionable (12–16). These fracture parameters determined from miniature dentine specimens, although useful as a first step, does not provide an understanding on how dental hard tissue

**Anil Kishen<sup>1</sup>, Ganesh V. Kumar<sup>1</sup>,  
Nah-Nah Chen<sup>2</sup>**

<sup>1</sup>Department of Restorative Dentistry, Faculty of Dentistry, National University of Singapore, Singapore 119074; <sup>2</sup>Department of Restorative Dentistry, National Dental Center, Second Hospital Avenue, Singapore 168938, Singapore

**Key words:** tooth fracture; crack propagation; dentine; stress; strain; fractography

Dr Anil Kishen, MDS, PhD, Department of Restorative Dentistry, Faculty of Dentistry, National University of Singapore, National University Hospital, 5 Lower Kent Ridge Road, Singapore 119074, Singapore  
Fax: +65 67732603  
e-mail: rsdak@nus.edu.sg

Accepted 15 October, 2003

anisotropy from a structural perspective resist catastrophic fractures.

This study aims to investigate some of these issues and to develop an understanding on the natural adaptation of dentine structure to fractures. This objective is achieved by computational finite element analysis; experimental tensile testing of dentine sections and fractographic investigations of clinically and experimentally fractured dentine. The current approach correlates stress–strain response and catastrophic fractures in dentine structure.

## Methods

The experiments were performed in three stages. In the first stage, a three-dimensional finite element analysis is conducted to evaluate the biomechanical response of dentine to tensile loading. In the second stage, tensile testing of dentine specimens was carried out. The tensile testing was used to observe the fracture response of dentine structure during tensile loading. In the third stage, fractographic evaluation is carried out with laser scanning confocal microscopy and scanning electron microscopy on clinically fractured post-core restored teeth specimens and experimentally fractured dentine specimens. The fractographs help in understanding failure patterns from fracture surface topography.

### Experiment 1: finite element analysis

In finite element analysis, the first step is the specification of elements. The elements are connected with each other at the nodes. The locations of nodes are defined using a three-dimensional coordinate system, which specifies the shape and size of the specimen model. Nodal points are also used to apply forces to the model. Based on the initial boundary conditions, the displacements at the nodes are determined for the given loads. The stress distribution and deformation are calculated from the nodal displacement using the stress–strain and strain–displacement relationships. In this analysis, a dentine section of length 10.0 mm, width 3.5 mm, and thickness 4.0 mm was modeled using 10-noded tetrahedron elements for the three-dimensional finite element analysis (Fig. 1). This formed one-half of the actual specimen used in the following experimental tensile testing. The finite element model of the dentine section included a circular root canal of 1 mm diameter along the length of the section. The dentine section was divided into seven material regions along the width.

In order to simulate the spatial gradients in elastic modulus of natural dentine, each material region in the model was assigned a different elastic modulus. The region representing the root canal was assigned an elastic modulus of 0.5 GPa and the region in the

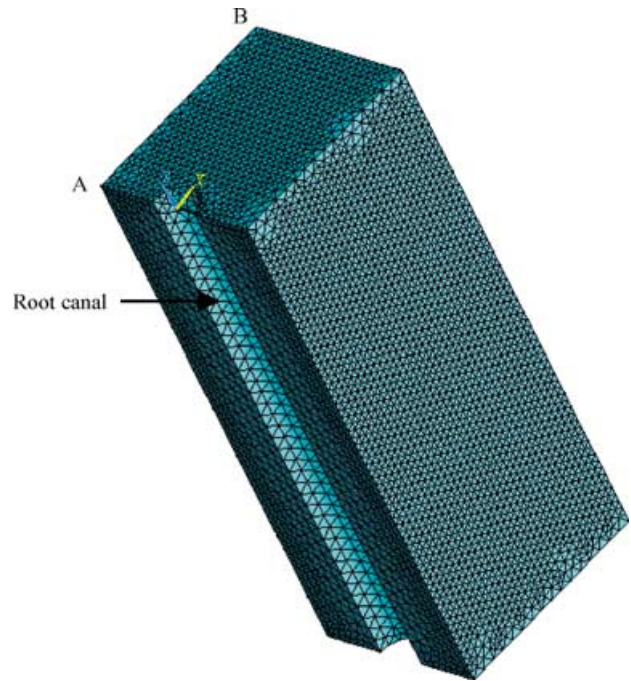


Fig. 1. Finite element discretization of the dentine block under unit uniform tensile load along the longitudinal direction.

outer periphery was assigned an elastic modulus of 12 GPa. In between the inner core and the outer periphery, five regions were assigned elastic moduli of 2, 4, 5, 7, and 10 GPa (inner to outer). This elastic modulus distribution was based on the results from our earlier microindentation experiments (13). A Poisson's ratio of 0.32 was assigned for the entire dentine structure (17). In this study, the following assumptions were made regarding the properties of tooth material and its geometry. (i) The sectional specimen was considered to be composed of dentine only. A cementum layer was not considered as the thickness of cementum was very small. (ii) Elastic modulus value of pulp was negligibly small when compared to dentine. Therefore, the effect of pulp on stress distribution was neglected and the pulp space was considered empty (17).

In the present model, interfaces with different material properties exist because of the step-wise simulation of elastic modulus. The interface region had a refined mesh of 0.15-mm node spacing transitioned to a coarse mesh of 0.25-mm node spacing in the inner region. Further, nodes were placed at a distance of 0.1 mm adjacent to the root canal wall. This facilitated accurate capture of strain values in the vicinity of the root canal. The three-dimensional finite element model consisted of 25 000 elements and 150 000 nodes. During testing, the finite element model was constrained at the bottom and a uniform unit tensile load was applied on the superior surface. A symmetrical displacement boundary condition was applied on

the plane of the root canal. This aided to simulate an actual specimen width of 8 mm. The ANSYS finite element program (Ansys Inc., Canonsburg, PA 15301, USA) was used to analyze stress and strain distributions in the three-dimensional meshed models.

#### Experiment 2: tensile testing

Six freshly extracted non-carious mandibular central incisor teeth were collected and stored in phosphate buffered saline (PBS) solution (0.1 M phosphate buffer, pH 7.2). These specimens were transilluminated so that teeth with cracks or extraction damage could be excluded from the study. Facio-lingual parallel-sided, slab-shaped (sagittal section) specimen of 3 mm thickness were prepared from each tooth. This was performed by grinding the specimens on wet emery paper (Presi, Grenoble, France) of grit sizes 180, 400, 800, and 1000 until the specimen surface was approximately 0.5 mm from the final desired plane. The specimens were then polished to the final finish using an automatic polisher (ECOMET-6, Buehler, USA) with 6 and 3  $\mu\text{m}$  particle-sized diamond paste (Presi, Grenoble, France). This manner of specimen preparation provided parallel, facial, and lingual sides for tensile testing, while preserving the major bulk of tooth dentine.

The specimens were randomly divided into two equal groups. A central notch was prepared on the facial side of specimens in group 1, while specimens in group 2 were tested without a notch. The notch in the group 1 specimens was prepared using a diamond disc. According to the British standards 5447 (18),  $a/W$  ratio must be in the range of 0.45–0.55, where  $a$  is the effective notch length and  $W$  is the width of the specimen (10). Based on this, the length and width of the notch prepared were 1.5 and 0.25 mm, respectively. During specimen preparation, constant water coolant was employed to prevent dehydration of dentine. The superior and inferior aspects of the specimens were trimmed off and aluminum tabs were glued on the edges of the specimen using araldite. This provided extra friction and more support for the test specimen. All specimens were stored at 37°C and 100% relative humidity for 24 h prior to testing.

A special miniature test grip was used to apply an axial tensile force, free from shear or torsion to the teeth specimens (Mini Mat, Rheometrics Inc., USA). The miniature material tester was set on a 0–200 N range with a 250 N load cell. The accuracy of the load cell was certified as better than 0.05%. During each test, a specimen was placed in the test grip and was subjected to tensile loads at a rate of 1 mm min<sup>-1</sup> (Fig. 2). The experimentally fractured specimens were later prepared for the fractographic analysis.

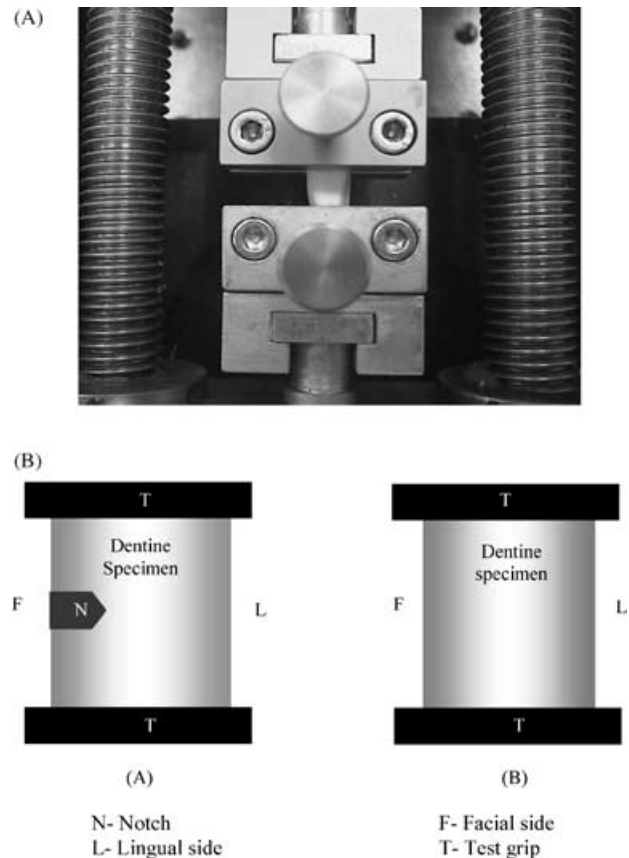


Fig. 2. (A) Shows the arrangement of the test specimen in the loading jig; and (B) schematic diagram showing the orientation of the specimen during tensile testing.

#### Experiment 3: fractographic analyses

##### *Clinically fractured specimens: case report 1*

In January 1999, root canal filling with lateral condensed gutta-percha and sealapex root canal sealer (Kerr, USA) was performed for a 43-year-old woman on upper right lateral incisor. The root canal treatment was uneventful, and a week later, a composite dental post (C-post, BISCO, USA) was placed in the coronal half of the root canal. The tooth was later prepared for full crown. A temporary crown was constructed, and a porcelain fused to metal crown was placed after 2 weeks.

In November 2000, the patient returned complaining of severe pain and gingival swelling for the past 3 days. Clinical examination revealed sensitivity to palpation and grade 3, Miller's mobility index on the upper right lateral incisor. A 6-mm pocket was measured on the buccal aspect of the associated tooth. Periapical radiograph revealed separation of root segment apical to the post. A definitive diagnosis of horizontal root fracture was made. The patient was informed about the fracture and advised to undergo extraction of the tooth (Fig. 3).



*Fig. 3.* Extracted incisor with horizontal root fracture in the clinical case 1.

*Clinically fractured specimens: case report 2*

In June 1999, acute apical periodontitis in relation to nonvital deeply carious left lower second molar was diagnosed in a 50-year-old woman. Subsequently, root canal treatment was performed on the tooth, using later condensed cold gutta percha and sealapex root canal sealer. Root canal treatments were uneventful. Two weeks later, the core built-up was performed using a Para-post (Whaledent, USA) on the distal canal and a self-threaded pin on the distally remaining intact dentine. The tooth was later prepared for full crown. A temporary crown was constructed and full metal crown (vitallium) was placed after 2 weeks.

In January 2000, the patient returned because of sudden pain. Upon clinical examination, a vertical fracture line on the buccal side of the left lower second molar tooth was noticed. A diagnosis of vertical root fracture of the left lower second molar was made and the tooth was extracted (Fig. 4).



*Fig. 4.* Extracted molar in the clinical case 2, showing the vertical fracture.

The selected clinical cases allowed examination of fracture topography without additional manipulation of dentine tissue. It was not the purpose of this investigation to study the contentious issue of why the post-endodontically restored teeth failed but to examine the clinically failed dentinal fracture surface topography.

*Experimentally fractured specimens*

The fractured specimens from tensile testing were examined under laser scanning confocal microscopy and scanning electron microscopy. This microscopic examination aided in relating the topographic features of the experimentally fractured dentine with the clinically fractured dentine.

**Results**

**Experiment 1: finite element analysis**

Figure 5(A) shows the normal stress distribution pattern in the dentine model along the loading direction (along the long axis of the tooth). The localized maximum tensile stress in the dentine model for unit tensile load was 4.59 GPa. In the FEM model, these stresses were observed along the outer surface of the dentine structure. Figure 5(B) shows the normal strain distribution in the dentine model along the loading direction. The localized maximum strain in the dentine model was 1.71. The highest tensile strain was located at a point in the inner core region of the dentine structure adjacent to the root canal.

Figure 6 shows the strain distribution along the longitudinal edge (plane perpendicular to the long axis of the tooth) between the inner core region adjacent to the root canal and the outer surface in the facio-lingual plane (between Fig. 1A and B). The strain indicated was for a unit uniform load applied on the plane parallel to the long axis of the tooth. It is found that the strain value was high in the dentine material adjacent to the root canal (at Fig. 1A), which steeply reduced to a very small value at about one-third the distance towards the outer surface (at Fig. 1B). The remaining dentine structure displayed low value of strains.

**Experiment 2: tensile testing**

It was observed that only two out of three specimens in group 1 and one out of three specimens in group 2 completely fractured during tensile loading for the maximum applied load of 200 N. It was also observed during the experiments that the complete fracture of the specimens occurred catastrophically from the notch tip at the facial surface to the lingual surface in the group 1. In group 2 specimens, the complete

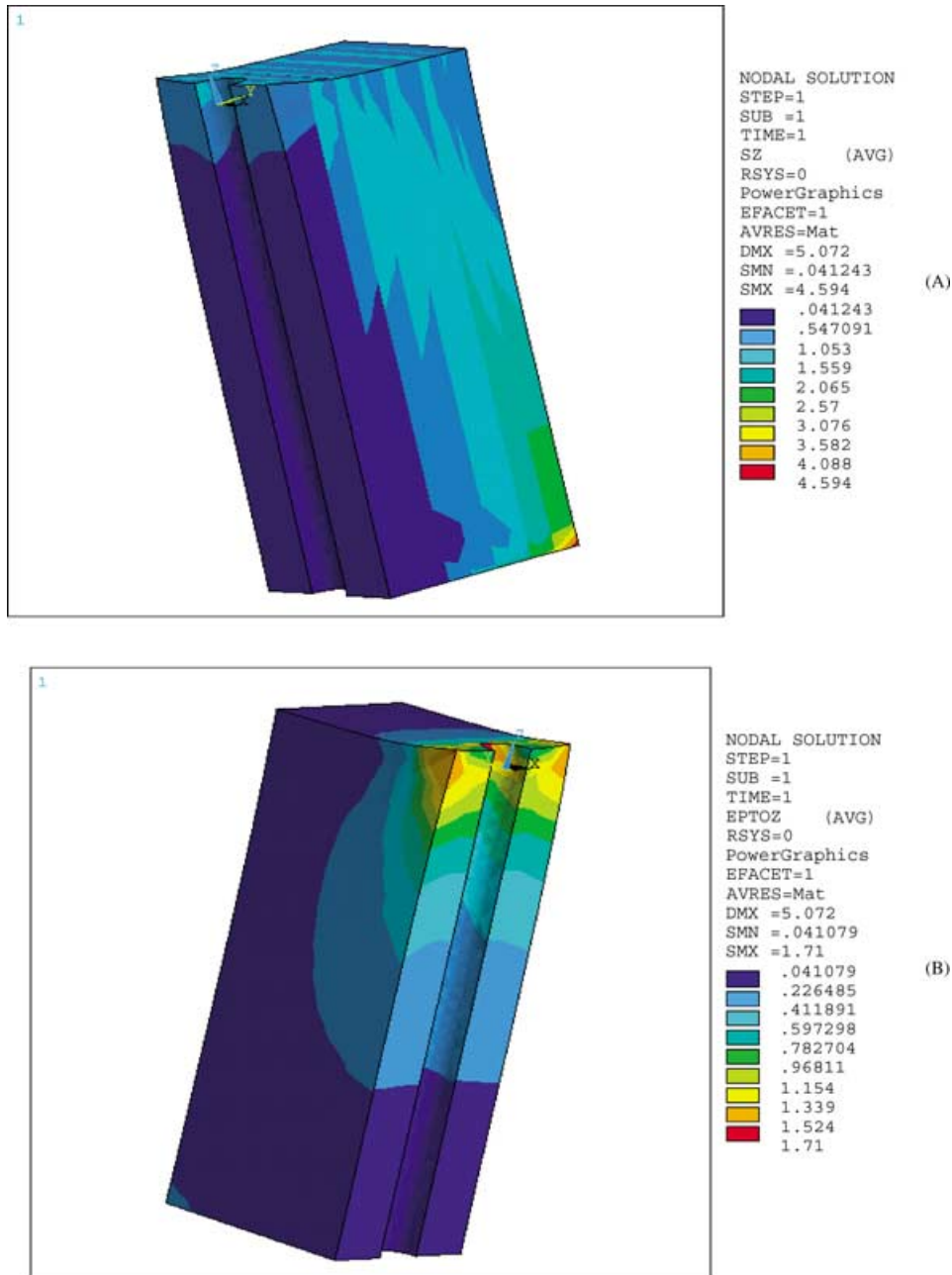


Fig. 5. (A) Shows the stress distribution (GPa), and (B) the strain distribution in the facio-lingual section of the dentine.

fracture progressed from the facial and lingual surfaces to the inner core region (Fig. 7).

### Experiment 3: fractographic analysis

#### *Clinically fractured specimens*

The laser scanning confocal microscopic and scanning electron microscopic examination revealed conspicuous fatigue markings on fractured dentinal surfaces. Significant numbers of cracks were observed on the dentinal surface of post-endodontically restored teeth. These cracks originated from

the inner region adjacent to the endodontic post and progressed predominantly towards the outer facial and lingual surfaces (Fig. 8B–C). Further, elongation of root canal orifice and a conspicuous deformation of adjacent inner dentine material were evident (Fig. 9A). A wide interfacial gap was noticed at the dentine–endodontic post interface and dentine–amalgam core interface (Fig. 8A). When the fracture topography was examined, it was observed that the inner dentine on the proximal (mesial and distal) sides of the root canal displayed ridge patterns (Fig. 9A), whereas the outer dentine on the facial

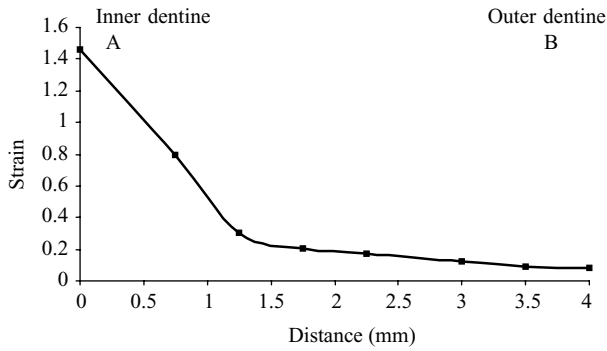


Fig. 6. Strain distribution in the dentine along the facio-lingual plane. The inner dentine (point A) and the outer dentine (point B) are indicated in Fig. 1.

and lingual side exhibited smooth fracture surfaces (Fig. 9B).

*Experimentally fractured specimens*

The laser scanning confocal microscopic and electron microscopic examination showed elongation of the root canal orifice in the facio-lingual direction. Increased deformation, corrugated topography, and microcracking were observed in the inner dentine material, around the root canal. The examination of the microcracks suggested that the initiation and progression of fractures in the dentine structure occurred from the inner region (adjacent to the root canal) to the outer surface of the tooth (Fig. 10A–C).

It was also observed from the fractographic analysis that the dentine in the inner region showed fracture progression perpendicular to the dentinal tubules (exposing the dentinal tubular orifices) and parallel to the dentinal tubules, whereas the fracture at the outer facial and lingual surfaces predominantly occurred parallel to the dentinal tubules (Fig. 10B).

Besides, the innermost dentine adjacent to the root canal exhibited microcracking and ridge patterns, which was characteristic of plastic deformations (Fig. 10C,D). It should be noted that microcracking and plastic deformation would result in reduced rate of crack propagation and increased fracture toughness (19).

**Discussion**

The major problem when dealing with biologic material from an engineering perspective is to know whether one is dealing with a material or a structure. Human dentine has ‘structure’ and yet is mostly treated as material. Previous studies have highlighted the spatial gradients in the material parameter such as stiffness in human dentine (13). In that case, the stiffness in dentine cannot be considered as a material parameter, and optimally attempt has to be made to model the structure (12). Differentiation between material and structure is crucial to better understand complex biologic material such as dentine.

Human dentine is a calcified tissue where the collagen-rich organic matrix is reinforced by calcium phosphate mineral particles. It is understood that mineralization and the spatial gradient of elastic modulus in human dentine is governed by the pattern of functional stress and strain distribution. This functional adaptation in dentine results in higher mineralization and larger elastic modulus in the outer dentine of the facio-lingual plane, while lesser mineralization (higher collagen) yields lower elastic modulus in the inner core dentine (Fig. 11) (13). This finding prompted us to consider the entire facio-lingual section of dentine structure for this analysis. Further, the lower mandibular central incisors are considered as they possess minimal bulk and mesial–distal width.

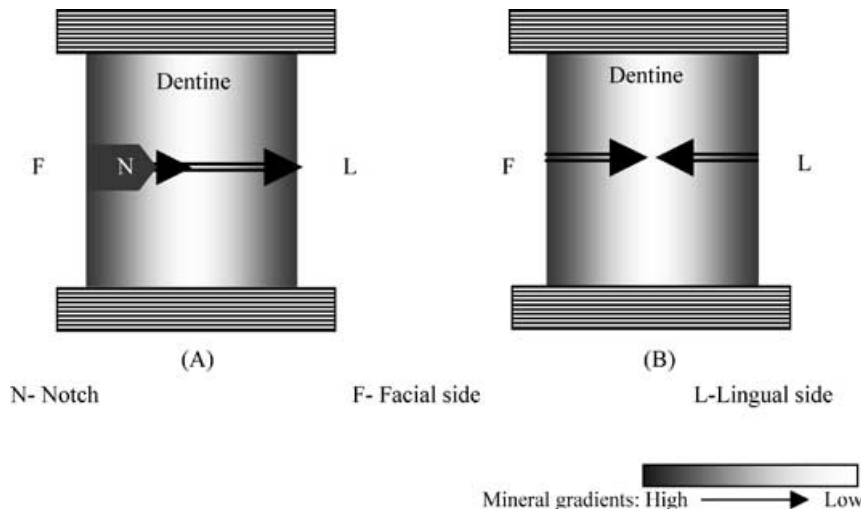


Fig. 7. Schematic diagram showing the pattern of progression of the catastrophic fracture in (A) group 1 and (B) group 2 samples.

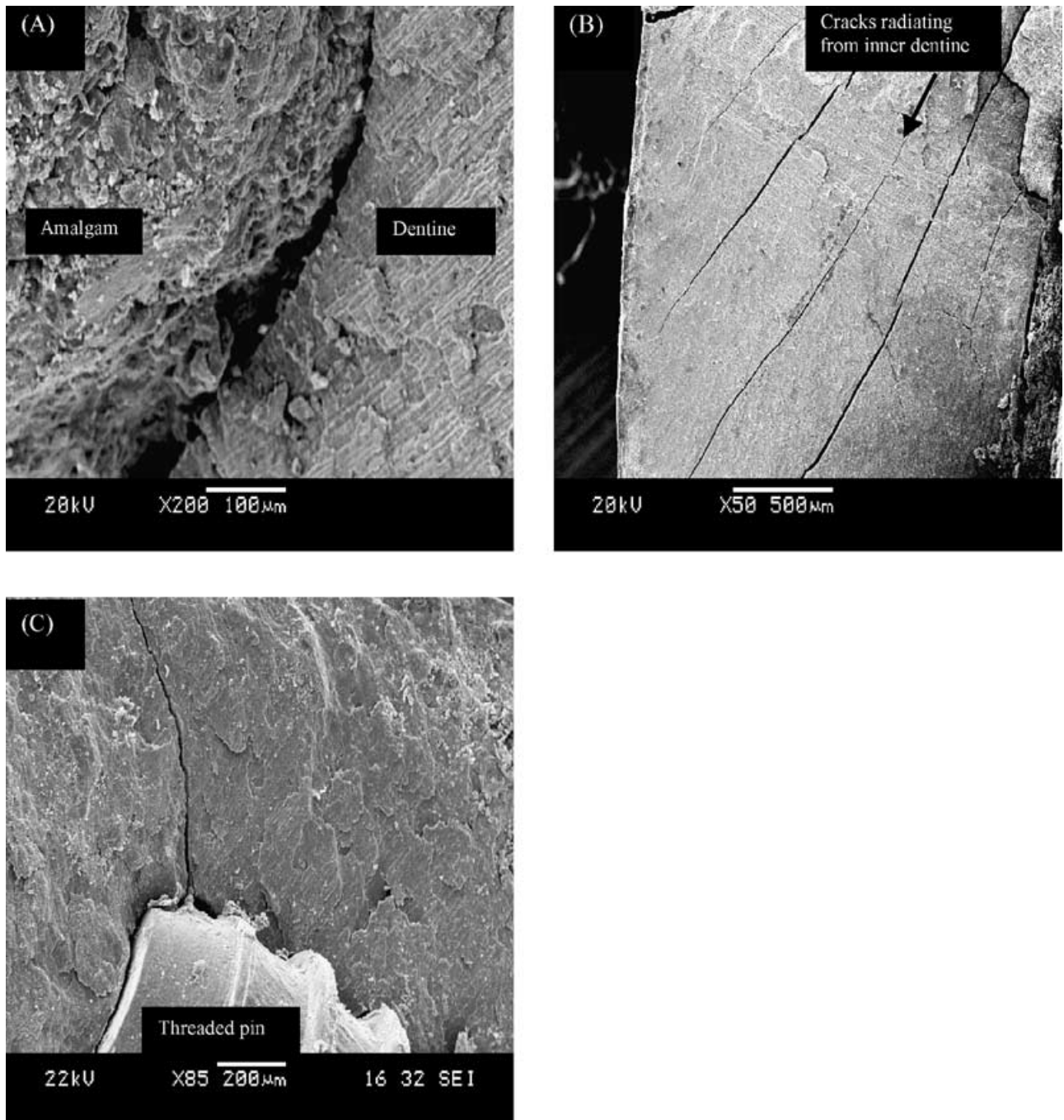


Fig. 8. Scanning electron microscopic images of the clinically fractured molar teeth specimens showing (A) the amalgam–dentine interface; (B) radiating cracks in the inner dentine; and (C) radiating crack in association with the threaded pin.

The results obtained from the tensile testing in this investigation demonstrated that the catastrophic fracture of dentine in group 1 progressed from the facial surface (adjacent to the notch tip) to the lingual surface, whereas in group 2, the catastrophic fracture of dentine progressed from the facial and lingual surfaces to the inner core region of the specimens. In addition, the fractographic examination of these specimens suggested that the microcracking and ridge

formation because of dentine deformation progressed from the inner core region to the outer surface. The finite element analysis displayed high strains and less stresses in the inner core region adjacent to the root canal, which consisted of less mineralized dentine with low elastic modulus. The finite element analysis also showed low strains and high stresses at the outer facial and lingual regions, which consisted of highly mineralized dentine with high elastic modulus. The

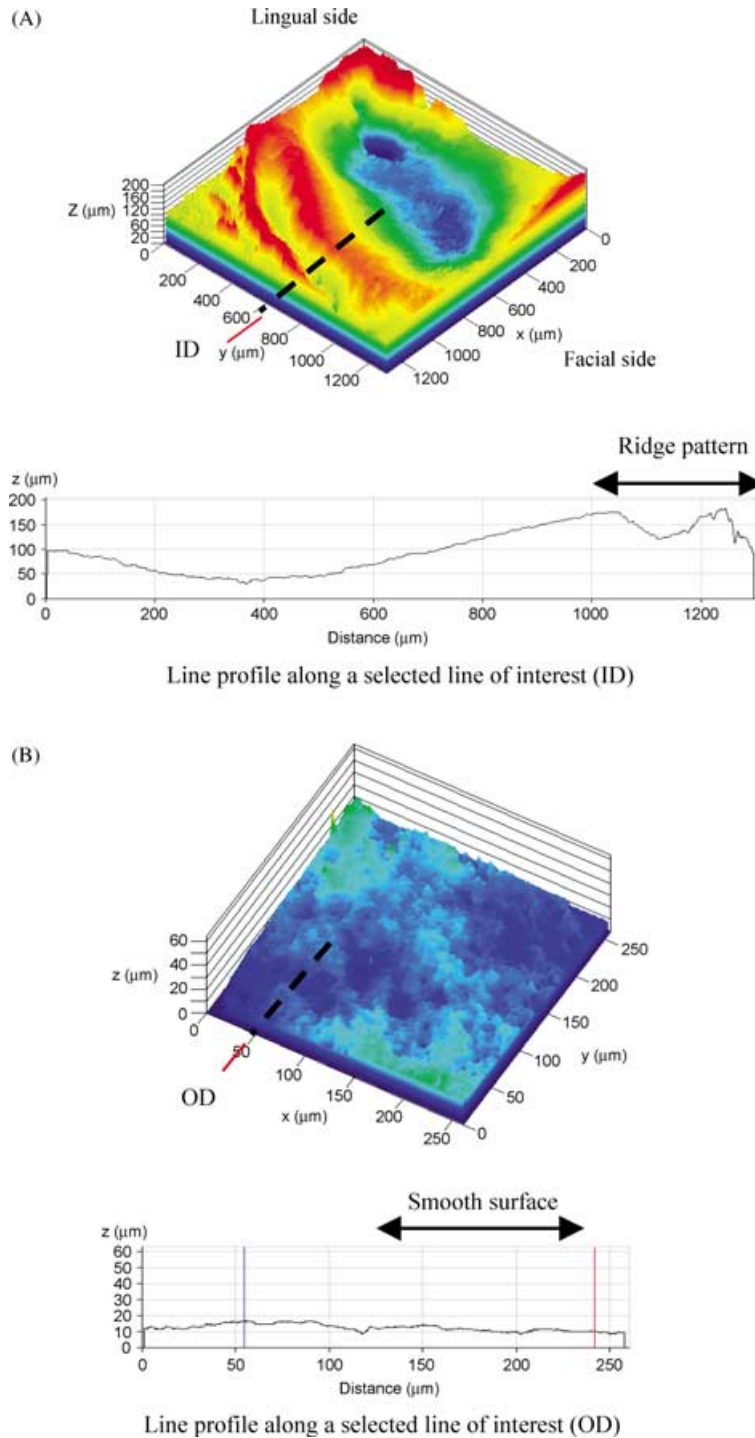
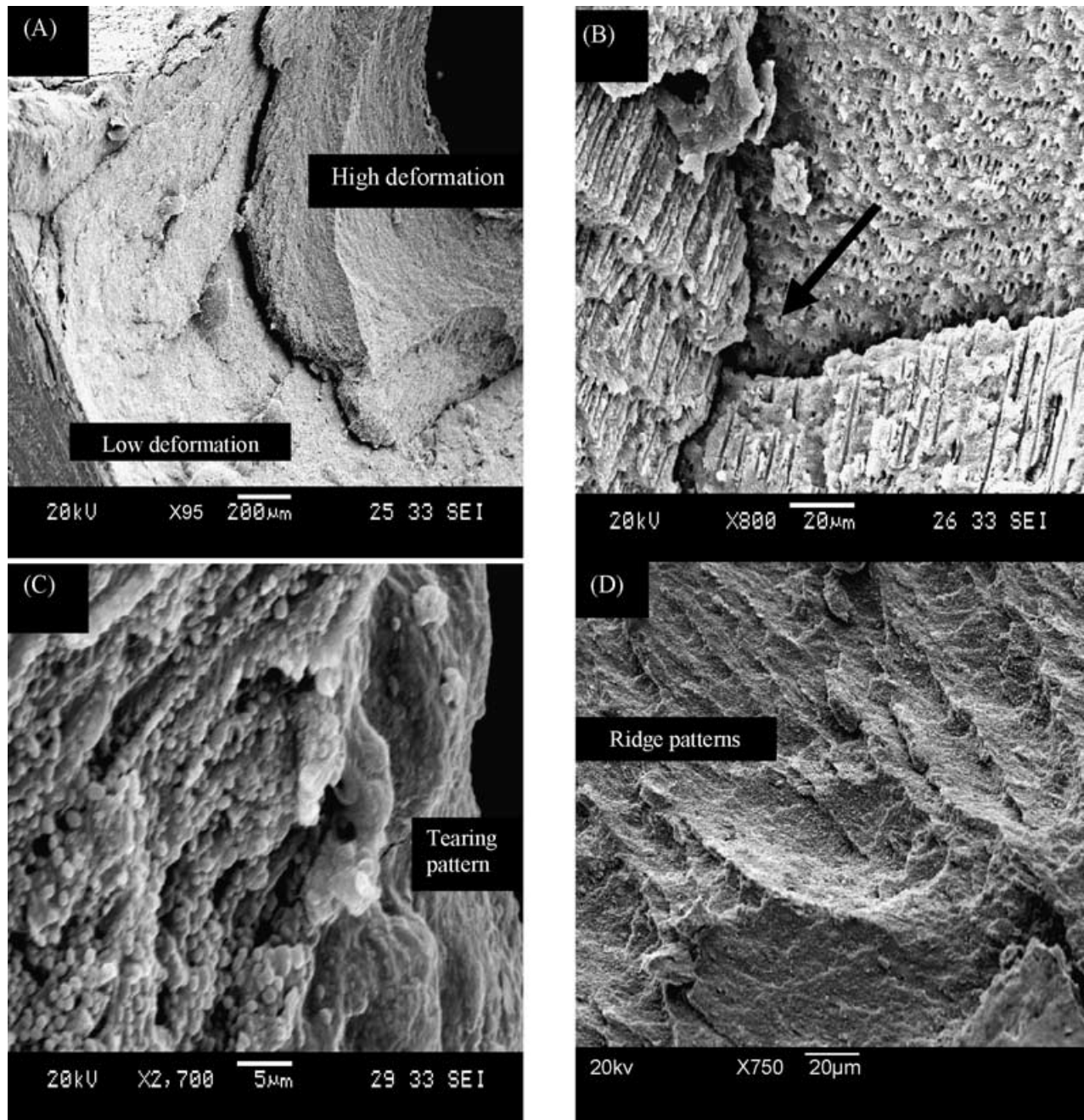


Fig. 9. Laser scanning confocal microscopic images of the clinically fractured incisor teeth specimen showing the topography of (A) inner dentine and (B) outer dentine.

variation in stress–strain distribution in the facio–lingual dentine can be primarily attributed to the distinct elastic modulus gradients in the dentine structure.

The fractographic analysis of the clinically fractured teeth specimens vividly showed that the clinically fractured dentine exhibited numerous microcrackings in the inner dentine. These

microcracks are more predominant in the region adjacent to the endodontic post. They originated from the inner dentine adjacent root canal and progressed towards the outer surfaces. This direction of progression of microcracks in clinically fractured teeth specimens are similar to the direction of microcracks observed in the experimentally fractured



*Fig. 10.* Scanning electron microscopic images of the experimentally fractured dentine specimens showing (A) deformed inner dentine; (B) dentine surface exhibiting fracture perpendicular and parallel to the dentinal tubules; (C) tearing pattern of dentine material adjacent to the root canal; and (D) ridge patterns in the inner dentine.

dentine. It is significant to mention that previous research based on fatigue and static analysis of post-core restored teeth also observed similar initial crack formation and initial failure in the inner dentine adjacent to the root canal (20, 21). They also suggested that these microcracks are impossible to detect clinically (22).

Having observed such a complex fracture behavior in dentine structure, and a distinct pattern of failures in fractured post-endodontically restored teeth, the

following paragraphs discuss how complexity in dentine improves its fracture resistance.

Engineering analysis has shown that the sharpness of the crack tip would govern stress concentration. The stress concentration would focus strain energy onto the next susceptible bond during crack propagation. However, at high strains during unidirectional extension, it is noted that the crack tip in the outer facial surface of the dentine has blunted. Fluoroscopic

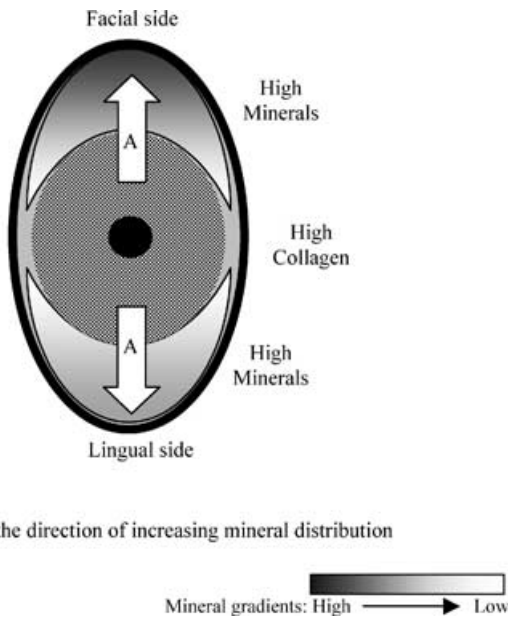


Fig. 11. Schematic diagram showing the mineral distribution pattern along the cervical cross-section in an incisor.

X-ray imaging of the dentine specimen that did not fracture completely at 200 N have confirmed this finding (15). This effect can be because of the natural spatial gradients in the elastic modulus of dentine, which grades from a stiff material at the open end of the notch to a less stiff material at the crack tip.

Transmissions of strain energy to the crack tip supplies energy for the crack propagation, and the speed at which the crack is fed with energy will depend upon the rate of change of shape of material adjacent to the crack (21). Consequently, the fracture resistance will be increased by any mechanism that increases the amount of energy required to propagate the primary crack. The microcracking and ridge patterns observed in the inner dentine are some of the many fracture-toughening mechanisms operating in the case of dentine (19). In structural dentine, high strains are experienced in the inner dentine, while high stresses are produced on the surface. This means that the energy fed into the structure as it is extended will be dissipated throughout the inner dentine with less possibility of a localized increase in stress at the surface. It should be emphasized that localize concentration of stresses at the surface can lead to catastrophic fracture of the structure (22).

The observed stress–strain response in the dentine is cited as the adaptive response of dentine as a structure to improve its fracture resistance. Additionally, it is of significance to note that the inner dentinal matrix, adjacent to the root canal, is less mineralized, and demonstrated high density of dentinal tubules (13, 23). Each dentinal tubule is generally filled with an odontoblast process, dentinal fluid (including

unbound water), collagen, and occasional nerves from the pulp (23). Collagen is a resilient biologic material that stores strain energy (12), while presence of water is found to significantly increase plastic deformation and fracture energy in dentine (19, 24). From a clinical perspective based on the above experiments, it is suggested that the conservation of inner dentine is crucial to offer toughness or fracture resistance to the tooth structure. Undue loss or removal of the inner dentine because of pathologic processes or during post and core restoration would compromise the toughness criteria in dentine structure, which in turn would predispose such tooth structure to catastrophic fractures. Furthermore, application of a morphologically designed dowel and core that minimizes excessive removal of inner dentine (9) and use of adhesive dental restorations are recommended to reinstate the natural stress–strain response in dentine structure.

**References**

1. Sorensen JA, Martinoff JT. Intracoronal reinforcement and coronal coverage: a study of endodontically treated teeth. *J Prosthet Dent* 1984;51:780–4.
2. Gutmann JL. The dentin-root complex: anatomic and biologic considerations in restoring endodontically treated teeth. *J Prosthet Dent* 1992;67:458–67.
3. Weine FS. *Endodontic therapy*, 5th edn. St Louis: Mosby; 1996. p. 756–801.
4. Helfer AR, Melnick S, Schilder H. Determination of the moisture content of vital and pulpless teeth. *Oral Surg Oral Med Oral Pathol* 1972;34:661–70.
5. Reeh ES, Messer HH, Douglas WH. Reduction in tooth stiffness as a result of endodontic and restorative procedures. *J Endod* 1989;15:512–6.
6. Carter JM, Sorensen SE, Johnson RR, Teitelbaum RL, Levine MS. Punch Shear testing. *J Biomech* 1983;16:841–8.
7. Guzy GE, Nicholls JL. *In vitro* comparison of intact endodontically treated teeth with and without endo-post reinforcement. *J Prosthet Dent* 1979;42:39–44.
8. Isidor F, Brondum K. Intermittent loading of teeth with tapered, individually cast or prefabricated, parallel-sided posts. *Int J Prosthodont* 1992;5:257–61.
9. Gluskin AH, Radke RA, Frost SL, Watanabe LG. The mandibular incisor: rethinking guidelines for post and core design. *J Endod* 1995;21:33–7.
10. El Mowafy OM, Watts DC. Fracture toughness of human dentine. *J Dent Res* 1986;66:677–81.
11. Rasmussen ST, Patchin RE, Scott DB, Heuer AH. Fracture properties of human enamel and dentin. *J Dent Res* 1976; 55:154–64.
12. Julian V. *Structural biomaterials*, revised edition. Princeton, New Jersey: Princeton University Press; 1990. p. 25–36.
13. Kishen A, Ramamurty U, Asundi A. Experimental studies on the nature of property gradients in human tooth. *J Biomed Mater Res* 2000;51:650–9.
14. Asundi A, Kishen A. *In vivo* strain and *in vitro* stress distribution in dental supporting structures – a strain gauge and photoelastic analysis. *Arch Oral Biol* 2000;45:543–50.
15. Kishen A, Asundi A. Fractographic investigations on human dentine. *J Dent Res* 2000;79:1324.
16. Tesch W, Eidelman N, Roschger P, Goldenberg F, Klaushofer K, Fratzl P. Graded microstructure and mechanical properties of human crown dentin. *Calcif Tissue Int* 2001;69:147–57.

**Kishen et al.**

17. Rubin C, Krishnamurthy N, Capilouto E, Yi H. Stress analysis of the human tooth using a three-dimensional finite element model. *J Dent Res* 1983;62:82–6.
18. British Standards 5447. Plane strain fracture toughness of metallic materials. London: British Standards Institution; 1977.
19. Kahler B, Swain MV, Moule A. Fracture-toughening mechanisms responsible for differences in work to fracture of hydrated and dehydrated dentine. *J Biomech* 2003;36:229–37.
20. Fan P, Nicholls JI, Kois JC. Load fatigue of five restoration modalities in structurally compromised premolars. *Int J Prosthodont* 1995;8:213–20.
21. Freeman MA, Nicholls JI, Kydd WL, Harrington GW. Leakage associated with load fatigue-induced preliminary failure of full crowns placed over three different post and core systems. *J Endod* 1998;24:26–32.
22. Kishen A, Asundi A. Photomechanical investigations on post-endodontically rehabilitated teeth. *J Biomed Opt* 2002;7:262–70.
23. Mjör IA, Sveen OB, Heyeraas KJ. Pulp-dentin biology in restorative dentistry. Part 1. Normal structure and physiology. *Quintessence Int* 2001;32:427–46.
24. Jameson MW, Hood JA, Tidmarsh BG. The effects of dehydration and rehydration on some mechanical properties of human dentine. *J Biomech* 1993;26:1055–65.